ENVIRONMENTAL SCIENCES 2000 Vol. 4, No. 3, 139~148
Bulletin of the Korean Environmental Sciences Society

Evaluation of DMS Flux and Its Conversion to SO_2 in Tropical ACE 1 Marine Boundary Layer

Zang-Ho Shon, Taekyung Yoon, and Jungkwon Kim

Department of Environmental Engineering, Dong-Eui University, Pusan

(Manuscript received on July 12, 2000)

A mass balance/photochemical modeling approach was used to evaluate the sea-to-air dimethyl sulfide (DMS) fluxes in tropical regions and part of the Southern Ocean. The flux determinations were based on 10 airborne observations by ACE 1 transit flights (i.e., Flights 4-9 and 29-32). The DMS flux values for the tropical regions ranged from 1.0 to 7.4 μmole/m^2/day with an average estimate of 4.2 ± 2.3 μmole/m^2/day. The seasonal variations in the DMS flux predicted for the equatorial Pacific Ocean based on atmospheric DMS measurements were not entirely consistent with those derived from seawater DMS measurements reported in previous literature. Inhomogeneities in the DMS flux field were found to cause significant shifts in the atmospheric DMS levels even in the same sampling location. Accordingly, no definitive statement can be made at this stage regarding systematic differences or agreements in the DMS flux estimates from the two approaches. Moreover, this study strongly suggests that DMS oxidation is the most likely dominant source of SO_2 in tropical regions, which is also supported by another set of compiled observations. Finally, these SO_2 observations indicate that, when significant data was available for both the boundary and buffer layers, the vertical SO_2 gradient between these two zones was primarily negative.

Key words : DMS, Flux, ACE 1, SO_2, overall conversion efficiency

1. Introduction

Oceanic emissions of dimethyl sulfide(DMS: CH_3SCH_3) are known to be a major primary source of natural sulfur in remote marine atmospheres[1~3], and SO_2, one of the oxidation products of DMS, is also recognized as a major source of sulfate aerosol. As such, the sulfate aerosol derived from the oxidation of DMS has the potential of influencing the Earths radiative budget, thereby defining an important climate forcing function[4]. This suggests that accurate assessments of both the DMS flux and its conversion efficiency to SO_2 and sulfate represent a critical input to future climate models.

Historically, the methods used to estimate DMS fluxes have fallen into two general categories: those based on seawater DMS measurements and those inferred from atmospheric observations. Of the two, flux determinations based on seawater DMS measurements have been the most extensively used. However, these determinations include substantial uncertainties, up to a factor of two, mainly due to parameterized transfer velocity[2~3]. The most frequently used atmospheric-DMS-based method is herein referred to as the mass balance/photochemical modeling(MBPCM) approach. The MBPCM method considers the mass balance between the DMS oceanic source and its atmospheric losses. As noted in [5] and [6], the potential uncertainties associated with the MBPCM approach include : 1) the availability of accurate primary oxidant levels, 2) a realistic parameterization of the vertical mixing, and 3) an accurate assessment of the boundary layer(BL) height.

The major sources of sulfur dioxide(SO_2) over remote ocean regions are believed to be the oxidation of DMS emitted from the ocean and entrainment of SO_2 from the buffer layer(BuL). Recent studies have suggested that the oxidation of DMS is the dominant source of SO_2 in the marine BL, whereas the entrainment of SO_2 from the free

troposphere only plays a minor role as an SO_2 source[7~10]. However, the efficiency of the DMS to SO_2 conversion process is still unclear, as noted in [5] and [6]. This paper presents an analysis of airborne sulfur data recorded during the transit flights of the first phase of the Aerosol Characterization Experiment(ACE 1) field study. This study explored the issue of DMS flux over the tropical Pacific Ocean plus the relative contribution of DMS oxidation to observed SO_2 levels in the marine BL.

2. Observational Data

This study used the data recorded during the transit flights of the ACE 1 field campaign. The ACE 1 campaign can be divided into two subgroupings : 1) intensive Southern Ocean flights(Flights 11-28) and 2) transit flights. Details concerning the intensive Southern Ocean flights have been previously described in [6] and [11]. Of the 31 marine flights(Flights 2-32) flown during ACE 1, ten of these(Flights 4-9 and 29-32) were made over the Pacific Ocean BL during Nov. through Dec., 1995. These flights covered a latitudinal range of 20°N to 60°S and a longitudinal range of 160°E to 156°W, as shown in Figure 1a. The commonly employed sampling strategy used by the *C-130* aircraft from the National Center for Atmospheric Research(NCAR) consisted of flying sequential circles(diameter ~60 km) at 3 or 4 constant altitudes (e.g., typically 30, 150, 300, 450, 600, and/or 900 m) while moving with the wind field. The sampling on each mission included both BL and BuL altitudes. For further details concerning all aspects of the ACE 1 sampling strategy, the reader is directed to the ACE 1 Overview paper by [11].

The ACE 1 field program included measurements of the sulfur species, DMS, SO_2, H_2SO_4, and MSA as well as the aerosol species, SO_4^{2-} and MS (methane sulfonate). It should be noted that DMS and SO_2 were also measured by the ship *Discoverer*. Other critical trace gases measured by the *C-130* aircraft included: OH, O_3, CO, CH_4, NO, H_2O_2, and CH_3OOH. All basic meteorological parameters were also recorded during each flight, including UV irradiance as measured by an Eppley radiometer.

The DMS and SO_2 measurements made by the *C-130* aircraft were made using a gas chromatography/mass spectrometry(GC/MS) technique in which isotopically labeled DMS and SO_2 were used as the internal standards. These standards, added to each individual sample, ensured that any sulfur losses in the cryogenic trap and sampling lines were properly corrected. Individual samples were first cryogenically trapped to preconcentrate the sample and then subsequently injected into a GC column. DMS and SO_2 were measured every 4-6 min(most typically 4 min.)

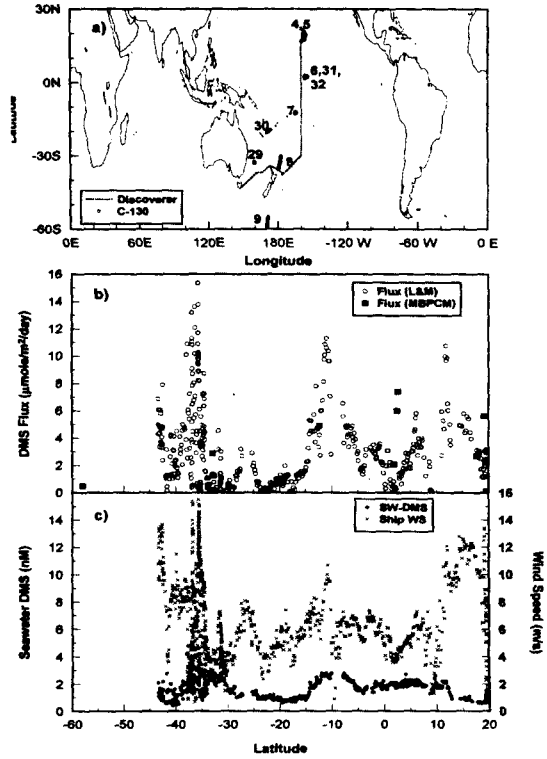

Fig. 1. a) North-south transect of research vessel Discoverer (dotted line) and flight track of C-130 research aircraft in MBL for transit flights during ACE 1. The numbers to next to the flight track are the flight numbers. b) comparison of DMS flux for transit flights estimated from MBPCM using air-sea exchange model (L&M). The air-sea exchange DMS fluxes were derived from measurements made on board the R/V Discoverer using piston velocity (L&M). c) The crosses and closed circles represent the wind speed and DMS concentration in the seawater measured on board the R/V Discoverer, respectively.

with a detection limit of ~1 parts per trillion by volume(pptv). For further details regarding this technique see [12] and [13]. For details on the measurements of other trace gases and aerosol species, the reader is directed to the ACE 1 "Overview" paper by [11].

During the transit flights of the ACE 1 program, the *C-130* aircraft sampled the BL 37 times, thereby producing 10 independent flux determinations. The reduction in the number of independent flux runs, reflects the fact that typically 3 or 4 BL runs from a given flight were used to make one independent flux determination.

The median concentrations of the photochemical species, NO, CO, H_2O, O_3, H_2O_2, CH_3OOH, and CH_4 formed the basis for all the input to the box modeling runs(see Table 1) which evaluated the diel profiles of OH and NO_3. As noted in [5] and [6], in the case of NO, most of the BL observations were at or below the 2σ detection limit of the onboard chemiluminescence NO sensor(e.g., typically 10-20 pptv for transit flights). Thus, the input to the model for NO involved bracketing possible values for NO as defined by assigning a lower limit value to the measurement of 1 pptv(labeled "Low-NO") and an upper limit value defined by the 2σ uncertainty for NO(labeled "High-NO"). This approach provided upper and lower limit values for OH. The DMS flux for these cases was estimated using an OH profile based on the average NO value as defined by the two values cited above.

3. Approach and Model Description

3.1 Approach

The method used in evaluating the DMS flux (F_{DMS}) in this work was based on the MBPCM approach, as described by [5], [14], and [15]. As outlined by these researchers, all forms of the MBPCM approach for determining the DMS flux require that the region under investigation has a reasonably high level of DMS horizontal homogeneity. Given the assumption that the BL is well mixed, the final form of the mass balance equation is as follows:

$$\frac{d[DMS]}{dt} = \frac{F_{DMS}}{EMD} - \left(k_{OH}[OH] + k_{NO_3}[NO_3]\right)[DMS] + \frac{1}{EMD}\int_{h_{BL}}^{h_{BML}} w\left(\frac{\partial[DMS(z)]}{\partial z}\right)dz \quad (1)$$

where EMD defines the DMS equivalent mixing depth (EMD) which can best be represented by expression (2) :

$$EMD = \frac{\int[DMS(z)]dz}{[DMS]_{BL}} \quad (2)$$

Table 1. Summary of Model Input Conditions

Flight Number	Sampling Time(local)	Latitude (negative : S)	Longitude (negative : w)	T[a] (C)	*Td[a] (C)	$[O_3]$[a] (ppbv)	[CO][a] (ppbv)	+[NO][a] (pptv)	$[NO_x]$[b] (pptv)	BL h (km)	EMD (km)
4	08 : 53	19.1	-157.4	22.5	18.2	34.4	97.1	10.7	77.2	0.7	1.1
5	10 : 12	17,7	-158.2	25.7	19.1	32.2	87.7	8.7	32.3	0.6	1.1
6	12 : 33	2.5	-155.0	23.0	18.1	25.4	78.9	6.7	23.6	1.0	1.0
7	13 : 08	-12.4	-165.0	26.2	22.2	14.1	70.0	4.8	17.0	0.6	1.3
8	13 : 29	-32.1	-178.1	18.5	15.7	24.0	95.6	4.1	16.8	0.2	0.4
9	12 : 28	-58.0	170.6	-2.9	-9.3	23.1	69.6	3.8	10.8	1.1	1.5
29	11 : 44	-32.7	159.2	20.1	11.0	21.4	61.2	4.4	12.4	0.7	1.2
30	13 : 21	-20.2	171.2	26.3	21.2	15.0	64.6	4.7	17.9	0.4	0.6
31	16 : 20	1.9	-156.4	22.5	18.1	9.8	68.8	2.6	6.3	0.5	1.0
32	10 : 39	2.9	-156.2	22.7	18.8	13.3	70.0	5.5	13.2	0.5	0.8

(a) Median observations ; (b) Model calculated quantity ; (*) Dew Point ; (+ For detail discussion on [NO], see context in section 3.

where $[DMS]_{BL}$ represents the average DMS concentration in the marine BL. The remaining terms in equation (1) include k_{OH} and k_{NO3}, the reaction rate coefficients for the reaction with OH and NO_3, respectively ; "w", the mean vertical velocity ; and $\partial[DMS(z)]/\partial z$, the vertical gradient of DMS within the BuL. From a practical point of view, the "best estimate" for F_{DMS} can be assessed by simply adjusting the flux value in equation (1) until the difference between the model-estimated and observed DMS profiles is minimized. The minimization routine used here was "chi-squared testing". For details concerning this equation see [6], [14], and [15].

Thereafter, the evaluated DMS flux can be used to generate a DMS diel profile for assessing the yield of the oxidation product SO_2. This evaluation is carried out using equation (3) which expresses the SO_2 mass balance resulting from the BL oxidized DMS and the loss of SO_2 from all the BL removal processes,

$$\frac{d[SO_2]_{BLDMS}}{dt} = \gamma\{ k_{OH}[OH] + k_{NO2}[NO_3][DMS] \} - L[SO_2]_{BLDMS} \quad (3)$$

It should be noted that "γ" in this equation represents the overall SO_2 conversion efficiency from the OH/NO_3/DMS reactions. As such, it defines the contributions from both the abstraction and addition channels of DMS oxidation. Equally important, the total first order SO_2 loss parameter, L, includes gas phase chemical losses and dilution by vertical transport as well as the physical removal processes defined by wet/dry ocean deposition, scavenging by sea-salt aerosol, and cloud droplets. The same SO_2 production efficiencies from DMS oxidation as those in [6] were used to calculate the BL SO_2 from DMS oxidation, $[SO_2]_{BLDMS}$. In brief, a "standard model" run was defined as using an SO_2 lifetime of 1 day coupled to a "best estimate" value for "γ" of 0.7. The lower and upper limits for the level of SO_2 were estimated based on the following "γ" and "L" combinations : = 0.7, 1/L = 0.25 days and = 1.0, and 1/L = 2 days. For further details concerning "γ", see [5] and [6].

3.2 Model Description

The sulfur chemistry model used in this study contained 14 reactions encompassing the sources and sinks for the sulfur species: DMS, DMSO, $DMSO_2$, MSIA, MSA, and SO_2. This model was then coupled to a full $HO_x/NO_x/CH_4$/NMHC time-dependent photochemical box model constrained by the measured values of NO, CO, O_3, H_2O, H_2O_2, CH_3OOH, and UV irradiance. Table 1 shows the input conditions of the full $HO_x/NO_x/CH_4$/NMHC time-dependent photochemical box model for the chemical species NO, CO, O_3, etc. as well as the meteorological parameters of temperature, dew points, latitude, etc. These were then used to define the diel profiles for OH and NO_3. The input conditions were defined by the median value for each parameter over several horizontal legs (typically 3 or 4) in the BL. NO_x was derived from the model calculations. Furthermore, when significant BL OH observational data was available at the time of the DMS observations, this was typically used to further constrain the model generated OH profiles by adjusting the critical J values. This sulfur chemistry model has been previously used to assess DMS sea-to-air fluxes as well as examine the oxidation products from DMS[14-16]. Details related to the $HO_x/NO_x/CH_4$/NMHC time-dependent photochemical box model have been previously described by [17]-[21].

4. Results and Discussion

The ACE 1 transit flights observations produced 10 independent BL DMS flux assessments. These are shown in Table 2 and Figure 1b. Flights 4 through 7 and 30 through 32 covered the tropical Pacific Ocean from 20°N to 20°S. Flights 8, 9, and 29 involved the Pacific Ocean at latitudes >33°S.

4.1. DMS Flux

4.1.1. Tropic

In Table 2 and Figure 1b, the individual DMS flux values range from 1.0 to 7.4 μmole/m^2/day, thereby producing an average estimate of 4.2 ± 2.3 μmole/m^2/day. Flights 4 and 5 were carried out over the tropical northern Pacific Ocean near Hawaii(21°N, 158°W) ; while Flights 7 and 30 were made over the tropical southern Pacific Ocean (see Figure 1a).

During late October and early November (for

Table 2. Sea-to-Air DMS Flux Estimates of Transit Flights

Flight Number	Date (1995)	Latitude (negative : S)	Longitude (negative : W)	Flux (μmole/m^2/day)
4	11/05	19.1	-157.4	5.4
5	11/06	17.7	-158.2	2.6
6	11/08	2.5	-155.0	6.0
7	11/10	-12.4	-165.0	5.3
8	11/11	-32.9	-178.4	2.7
9	11/14	-58.0	-170.6	0.5
29	12/16	-32.7	159.2	1.3
30	12/18	-19.9	172.0	1.0
31	12/19	1.9	-156.4	1.8
32	12/20	2.7	-156.2	6.7

about 3 weeks), the north-south transect of the ship *Discoverer* and the *C-130* aircraft (e.g., Flights 4-8, 31, and 32) covered a similar geographical area. As a result, Figure 1b shows a comparison of the DMS fluxes derived from the MBPCM approach with those based on [22]'s piston velocity (or transfer velocity) formulation. Even though the seawater DMS measurements were not made at the same time and location as the *C-130* aircraft measurements, the MBPCM derived DMS fluxes were reasonably consistent with the seawater DMS derived fluxes, except for Flights 4, 6, and 32. The higher seawater-DMS-based fluxes near 40°S and 10°S were the result of a combination of higher wind speed and seawater DMS levels(see Figure 1c).

As discussed in [6], most of the BL NO observations were at or below the 2σ detection limit of the on-board chemiluminescence NO sensor. Flights 4 and 5 had a very large 2σ uncertainty of 10-20 pptv when compared with that for the Southern Ocean flights (e.g., ~5 pptv for Flights 11-28). The DMS fluxes estimated for Flights 4 and 5 thus varied from 1.7 to 8.7 μmole /m^2/day and 1.1 to 4.0 μmole/m^2/day, respectively, depending on which detection limit value was assigned to NO(i.e., "High-NO" or "Low-NO"). For Flights 4 and 5, the lower limit values of the MBPCM derived DMS fluxes were closer to the seawater-DMS-based fluxes (L&M, Liss and Merlivat 1986). According to a recent DMS flux study by [23], BL NO levels of 3 pptv measured during September near Hawaii were close to the lower limit value for NO found during ACE 1.

As shown in Figure 1a, the BL runs of Flights 6, 31, and 32 were sampled near the equator(e.g., 2°N to 3°N near Christmas Island). The DMS flux for Flight 31 was significantly lower than those recorded by Flights 6 and 32, and although there was a sampling time gap of 1.5 month, Flights 6 and 32 still showed a similar magnitude DMS flux. These three flights, however, were insensitive to the assigned value for NO. The large difference (by a factor of 3.7) in DMS fluxes between Flights 31 and 32 would appear to be at least partially due to a difference in the meteorological conditions (i.e., wind speed) and partially due to seawater DMS changes. Since surface wind speed observations near Christmas Island during the time period of ACE 1 Flights 31 and 32 are unavailable, wind speed observations recorded in the lowest horizontal legs of the aircraft flight pattern were used. These were measured at altitudes of about 70 and 55m, respectively. Based on the vertical profile of the wind speed recorded during the descents and ascents, the wind speed patterns for these two flights appeared quite similar. The median wind speed for Flight 32 (9.7 m/s) was 40% higher than that for Flight 31 (6.9 m/s). The wind speed contribution to the DMS flux difference between Flights 31 and 32 was calculated using [22]'s piston velocity parameterization with an adjustment for the effect of temperature on the molecular diffusivity, which involved the use of Schmidt number derived from the empirical equation developed by [24]. As a result, the difference in the DMS flux due to a wind speed change was about a factor of 1.8. Based on this assessment, wind speed change accounted for 50% of the DMS flux difference between Flights 31 and 32. The remaining 50% possibly involved variations in the seawater DMS concentration, however, this unexplained portion is still within the uncertainty range of the piston velocity parameterization by [22].

The DMS flux estimates near Christmas Island during ACE 1 were consistent with previous independent estimates by [8] and [14]. [14] reported a DMS flux of ~3.3 $\pm$ 1.9 μmole/m^2/day at Christ-

mas Island estimated using the airborne-DMS-measurement-based method (i.e., MBPCM) during the late summer of 1996 during NASA's GTE PEM-Tropics A program. [8] reported a DMS flux of 3.2-6.5 μmole/m^2/day with a mean value of 5.2 μmole/m^2/day estimated using ground-based DMS measurements during the summer of 1994. [15] also calculated the DMS flux over Christmas Island using [8]'s database and arrived at a value of 4.9$\pm$ 1.7 μmole/m^2/day when using the MBPCM approach.

The seasonal variations in the DMS flux predicted for the equatorial Pacific Ocean, based on atmospheric DMS measurements[7,8,14,15,23,25,26] were not entirely consistent with those derived from seawater DMS measurements reported in previous literature(1972-1996) ([27] and references therein), as shown in Figure 2. The seawater-DMS-based fluxes were calculated using seawater DMS and [22] and [28]'s transfer velocity formulations in which the wind speeds were derived from local in-situ values and daily mean values provided by the NOAA-CIRES Climate Diagnostic Center. The seawater DMS data sets were typically averaged

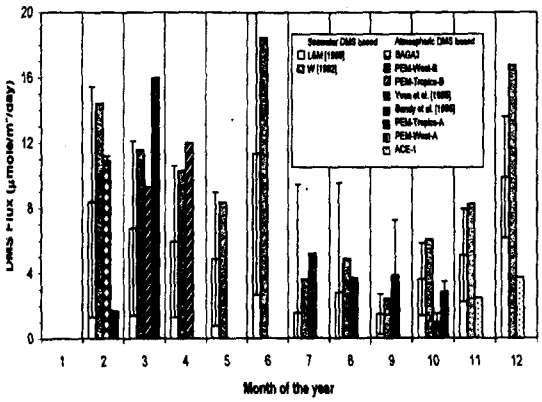

Fig. 2. Monthly DMS fluxes for equatorial Pacific regions (15°S-15°N). The DMS fluxes were calculated based on seawater and atmospheric DMS measurements. L&M(1986) and W(1992) indicate the DMS flux estimated based on the seawater DMS and parameterized transfer velocity of Liss and Merlivat (1986) and Wanninkhof (1992), respectively. The legends under atmospheric DMS based indicate field experiments that estimated the DMS fluxes based on atmospheric DMS measurements.

over 6 hours. In addition, Figure 2 shows that the maximum seawater-DMS-based fluxes occurred during the summer (except for June) with the minimum occurring during the winter. In contrast, the atmospheric-DMS-based fluxes during Feb-Apr were significantly higher than in any other season by a factor of more than 2. This inconsistency in the seasonal variation of the DMS flux most likely resulted from comparing relatively short-term observations under the airborne program with more long-term seawater DMS observations.

The trend in the atmospheric DMS concentration over the tropics was similar to that of the DMS flux. In other words, higher DMS concentrations were found over the equatorial regions. Figure 3 shows the DMS concentrations near Christmas Island based on both airborne and ground-based measurements. The atmospheric DMS concentrations for Flights 6 and 31 were within the diurnal range of the ground-based DMS measurements at Christmas Island as reported by [8] for summer conditions. They were also consistent with the Flight 6 levels observed during PEM Tropics-A[14], yet somewhat higher than those for Flight 7 of PEM Tropics-A. The latter flight, however, was greatly influenced by the presence of a significant shallow convection. In addition, the atmospheric DMS concentrations for Flight 32 of ACE 1 were significantly higher than those for Flight 31 of ACE 1 by a factor of more than 3 within 2 days, as noted in the DMS flux difference between Flights 31 and 32. Possible causes for the difference in the atmospheric DMS levels could be assigned to several areas including the OH levels, BL height, and inhomogeneity in the DMS flux field. However, the BL height and OH levels alone could not explain the significant changes in the atmospheric DMS levels. The BL heights for both Flights 31 and 32 were similar (e.g., 0.5km), yet the OH levels did have an impact on the atmospheric DMS difference because the OH level for Flight 32 was higher by a factor of 1.4.

Simulations to assess the effect of inhomogeneities in the DMS flux field (i.e., a dramatic change in the seawater DMS and wind speed) on the atmospheric DMS levels were also explored. In these simulations, it was assumed that the sampling location for Flight 31 was resampled 42 hours after horizontal advection had moved the DMS from

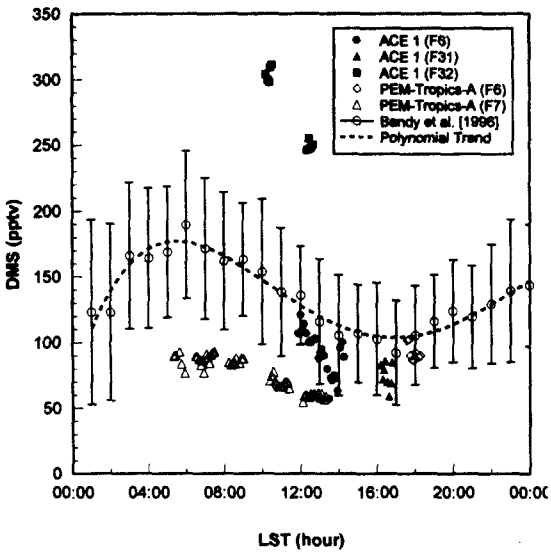

Fig. 3. Atmospheric DMS concentrations near Christmas Island based on airborne measurements (ACE 1 and PEM-Tropics-A) and ground-based measurements (Bandy et al. 1996).

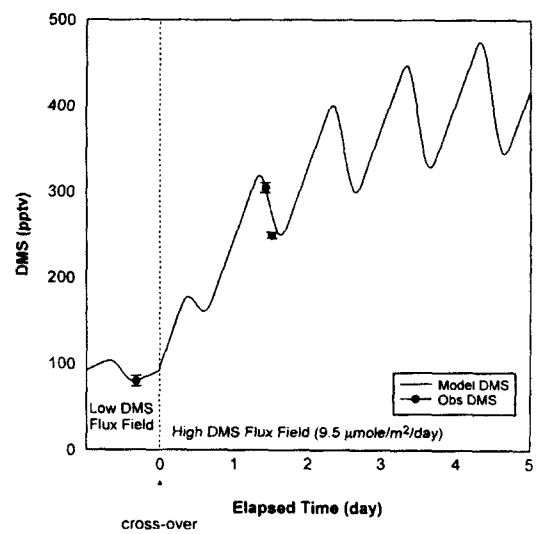

Fig. 4. DMS evolution after perturbation in DMS flux field until DMS reaches new quasi-steady state. A DMS flux of 9.5 μmole/m^2/day was required to reach the observed DMS levels 42 hours after perturbation. The filled circles in the low DMS flux field are the DMS concentrations recorded by Flight 31, whereas those in the high DMS flux field are the DMS concentrations recorded by Flight 32.

a higher flux field into the same location. As a result Figure 4 shows that the required DMS flux was 9.5 μmole/m^2/day 42 hours after the perturbation. In this simulation, the difference in the DMS lifetime between Flights 31 and 32 was not considered. The cross-over time for an air parcel going from the first to the second flux field was assumed to occur at midnight, as when compared to the DMS flux field change occurring at midday, the required DMS flux was slightly lower due to the build-up of DMS during the nighttime. However, when the lifetime difference was considered, the required DMS flux was reduced to~6μmole/m^2/day. This value was similar to the DMS flux for Flight 32. Consequently, inhomogeneities in the DMS flux field would appear to cause significant shifts in the atmospheric DMS levels even in the same sampling location.

4.1.2. Southern Ocean Transit Flights

The BL sampling runs for transit Flights 8, 9, and 29 were carried out over the Southern Ocean. Flight 9 was the southernmost flight (58°S) during ACE 1. Although this flight was geographically close to the intensive Southern Ocean study area (40°S-55°S), it was not grouped with the intensive Southern Ocean flights (Flights 11-28) due to a temporal difference. The BL sampling runs for Flights 8 and 29 were at similar locations (~33°S). In general, the DMS fluxes for these three transit flights were consistent with those derived from the intensive study over the Southern Ocean (see [6]). For example, the DMS flux of 0.5 0.3 μmole/m^2/day recorded by Flight 9 was quite similar to those of flights made further south (e.g, Flights 11 and 16) in the Antarctic zone. The DMS fluxes measured by Flights 8 and 29, located north of the subtropical convergence zone (STCZ), were also within the range of the DMS fluxes measured for the STCZ. As shown in Figure 1b, the MBPCM fluxes for these three flights were consistent with the L&M fluxes, although the *C-130* track for Flight 29 was slightly off the *Discoverer* transect (see Figure 1a). When compared to the tropical regions during ACE 1, the DMS fluxes recorded by transit flights 8, 9 and 29 were relatively low.

4.1.3. DMS Flux Sensitivity Analysis

Model sensitivity calculations for ACE 1 were previously carried out for each major variable in

equation (1), i.e., OH, observed DMS, NO_3, and $\int w(\partial DMS/\partial z)dz$, as noted in [6]. This procedure involved increasing and then decreasing the value of each variable by a factor of 2 and then examining the effect on the calculated flux. The sensitivity of each variable, OH, observed DMS, NO_3, and $\int w(\partial DMS/\partial z)dz$, was $+2/-2$, $+1.8/-1.7$, $+1.9/-1.7$, $+1.2/-1.1$, and $\pm$~1, respectively. These were similar to other results reported earlier by [6], [15], and [23]. The accuracy in defining the photochemical environment, vertical gradient in the DMS, and homogeneity of the DMS flux field is most critical in minimizing potential systematic errors in the MBPCM approach. For the 10 DMS flux estimates reported here, the lack of a homogeneous DMS flux field was most likely the major source of error.

The magnitude of the random error associated with each MBPCM DMS flux determination was estimated using an error propagation analysis. The resulting values ranged from 20 to 80%, with an average value of 50%. The three major contributors to this overall error included the OH, observed DMS, and EMD at 32, 9, and 10%, respectively. The error associated with OH was primarily related to the uncertainty in estimating the cloud correction factor as clouds were often encountered during the ACE 1 airborne sampling program. The uncertainty specified for the value of the observed DMS primarily reflected the atmospheric fluctuations of this species rather than any inherent instrument precision problems in measuring DMS. As regards the final parameter, EMD, the uncertainty in defining the BL height and in accurately assessing the vertical gradient in the DMS contributed equally to the overall error.

4.2. Contribution of DMS oxidation to BL SO_2

Figure 5 shows a comparison of the observed SO_2 values with those from the model simulations. As discussed in section 3.1, for the transit flights, the same simulation conditions as the "intensive" Southern Ocean flights of ACE 1 (see [6]) were used to study the contribution of DMS oxidation to the observed BL SO_2 levels. Of those transit flights considered, Flights 4, 5, and 30 were excluded from the analysis because of the influence of the Kilauea volcanic plume.

For 2 out of 4 tropical flights (e.g., Flights 6, 7, 31, and 32), the standard case values of $[SO_2]_{BLDMS}$ were higher than those observed. For the last 2 sampling events (e.g., Flights 7 and 31), the standard case still showed the calculated SO_2 values as 50% higher than the observations. Accordingly, these results strongly suggest that DMS oxidation is also the most likely dominant source of SO_2 in tropical regions. This conclusion was also supported by another set of compiled observations. These SO_2 observations indicated that when significant data was available for both the BL and the BuL, the vertical SO_2 gradient between these two zones was primarily negative. This was also corroborated in a sulfur study near Christmas Island reported by [8] and [14]. In these studies, a strong anti-correlation was found between DMS and SO_2, i.e., systematic decreases in DMS were seen following sunrise along with systematic increases in SO_2. Since there were only 3 flights

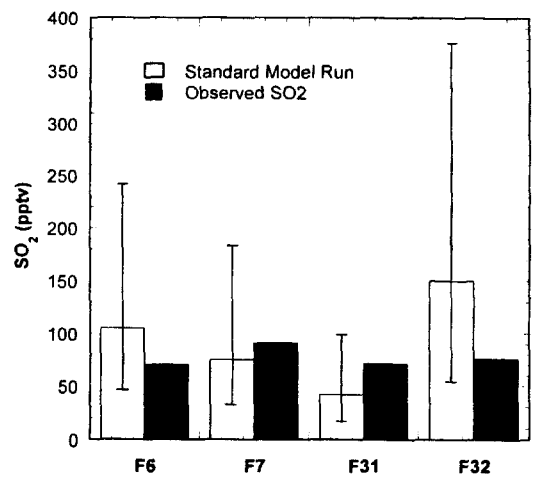

Fig. 5. Comparison of observed SO_2 with model simulated values during ACE 1 transit Flights 6-7 and 31-32. The symbol "γ" defines the overall DMS to SO_2 conversion efficiency and τ is the SO_2 lifetime. The top and bottom of each vertical line define the upper and lower limit model estimates for the mixing ratio of SO_2 when produced from DMS. These limits correspond to γ and τ values of 1.0 and 2 days versus 0.7 and 0.5 days, respectively. The best estimate is defined above the clear rectangular bars and corresponds to $\gamma = 0.7$ and $\tau = 1$ day. The mixing ratios observed for SO_2 are defined above the solid rectangular bars.

among the ACE 1 transit flights over the Southern Ocean, the statistical robustness of these results is questionable. Therefore, for a more detailed analysis of the Southern Ocean, the reader is directed to the intensive flight sequence over the Southern Ocean by [6].

5. Summary and Conclusion

The MBPCM approach was used to evaluate the sea-to-air DMS fluxes for tropical regions and part of the Southern Ocean. The flux determinations were based on 10 airborne observations recorded by ACE 1 transit flights (i.e., Flights 4-9 and 29-32). The first half of these occurred in November and the second half in the middle of December. The latitude range covered by the flights was 20°N to 60°S. The DMS flux values for the tropical regions ranged from 1.0 to 7.4 μmole/m^2/day, resulting in an average estimate of 4.2 ± 2.3 μmole/m^2/day. The DMS fluxes over the Southern Ocean during the transit flights were also found to be consistent with those derived from the intensive study period.

Although a comparison of the transit flights MBPCM results with ship-derived DMS flux values did not demonstrate any major systematic differences between the two methods, no definitive statement can yet be made regarding either the systematic differences or the agreement between these two approaches. This merely reflects the fact that the conditions under which the comparisons were made were far from the ideal.

The seasonal variations in the DMS fluxes for the equatorial Pacific Ocean, based on atmospheric DMS measurements, were not entirely consistent with those derived from seawater DMS measurements reported in previous literature. This inconsistency in the seasonal variation of the DMS flux probably resulted from comparing relatively short-term observations under the airborne program with more long-term seawater DMS observations. The trend in the atmospheric DMS concentration over the tropics was similar to that of the DMS flux, with higher DMS concentrations over the equatorial regions. Inhomogeneities in the DMS flux field were found to cause significant shifts in the atmospheric DMS levels even in the same sampling location.

Out of the 10 BL sampling events over the tropical regions and part of the Southern Ocean, 4 runs in the tropics were analyzed. For 2 of these 4 runs, the standard case values of SO_2 produced from DMS were higher than the observations. For the other two sampling events, the standard case still showed the calculated SO_2 values to be 50% higher than the observations. Accordingly, this study advocates that the DMS oxidation over the tropics is the dominant source of SO_2.

Acknowledgements

The author would like to acknowledge the partial support of this research by the U.S.A. National Science Foundation under grant ATM-9617378. I would also like to thank Drs. Doug Davis and Gao Chen for many informative discussions. This research is a contribution to the International Global Atmospheric Chemistry (IGAC) Core Project of the International Geosphere-Biosphere Program (IGBP) and part of the IGAC Aerosol Characterization Experiment (ACE).

References

[1] Andreae, M. O. and H. Raemdonck, 1983, Science, 221, 744~747.

[2] Andreae, M. O., 1986, In The Role of Air Sea Exchange in Geochemical Cycling, D. Reidel, Netherlands, pp 331~362.

[3] Bates, T. S., J. D. Cline, R. H. Gammon, and S. R. Kelly-Hansen, 1987, J. Geophys. Res., 92, 2930~2938.

[4] Charlson, R. J., J. E. Lovelock, M. O. Andreae, and S. G. Warren, 1987, Nature, 326, 655~661.

[5] Shon, Z.-H., 1999, Ph. D. Dissertation, Georgia Institute of Technology, Atlanta, Georgia, USA.

[6] Shon, Z.-H., D. Davis, G. Chenl, G. Grodzinsky, A. Bandy, D. Thornton, S. Sandholm, J. Bradshaw, R. Stickel, W. Chameides, G. Kok, L. Russell, L. Mauldin, D. Tanner, and F. Eisele, 2000, Atmos. Env., In print.

[7] Yvon, S. A., E. S. Saltzman, D. J. Cooper, T. S. Bates, and A. M. Thompson, 1996, J. Geophys. Res., 101, 6899~6909.

[8] Bandy, A. R., D. C. Thornton, B. W. Blomquist, S. Chen, T. P. Wade, J. C. Ianni, G. M. Mitchell, and W. Nadler, 1996, Geophys. Res. Lett., 23, 741~744.

[9] Davis, D. D., G. Chen, A. Bandy, D. Thornton, F. Eisele, L. Mauldin, D. Tanner, B. Huebert, and A. Clarke, 2000, Geophys. Res. Lett., To be submitted.

[10] Chen, G., D. D. Davis, P. Kasibhatla, A. R. Bandy, D. C. Thornton, B. J. Huebert, and A. D. Clarke, 2000, submitted to J. Geophys. Res.

[11] Bates, T. S., B. J. Huebert, J. L. Gras, F. B. Griffiths, and P. A. Durkee, 1998, J. Geophys. Res., 103, 16297~16318.

[12] Bandy, A. R., D. L. Scott, B. W. Blomquist, S. W. Chen, and D. C. Thornton, 1992, Geophys. Res. Lett., 19, 1125~1127.

[13] Bandy, A. R., D. C. Thornton, and A. R. Driedger III, 1993, J. Geophys. Res., 98, 23423~23433.

[14] Davis, D. D., G. Chen, A. Bandy, D. Thornton, F. Eisele, L. Mauldin, D. Tanner, D. Lenschow, B. Huebert, J. Heath, A. Clarke, and D. Blake, 1999, J. Geophys. Res., 104, 5675~5784.

[15] Chen, G., D. Davis, P. Kasibhatla, A. Bandy, D. Thornton, B. J. Huebert, and A. D. Clarke, 1999, J. Geophys. Res., 104, 5471~5482.

[16] Davis, D. D., G. Chen, P. Kasibhatla, A. Jefferson, D. Tanner, F. Eisele, D. Lenschow, W. Neff, and H. Berresheim, 1998, J. Geophys. Res., 103, 1657~1678.

[17] Davis, D. D., G. Chen, W. Chameides, J. Bradshaw, S. Sandholm, M. Rodgers, J. Schendal, S. Madronich, G. Sachse, G. Gregory, B. Anderson, J. Barrick, M Shipham, J. Collins, L. Wade, and D. Blake, 1993, J. Geophys. Res, 98, 23501~23523.

[18] Davis D. D., J. Crawford, G. Chen, W. Chameides, S. Liu, J. Bradshaw, S. Sandholm, G. Sachse, G. Gregory, B. Anderson, J. Barrick, A. Bachmeier, J. Collins, E. Browell, D. Blake, S. Rowland, Y. Kondo, H. Singh, R. Talbot, B. Heikes, J. Merrill, J. Rodriguez, and R. E. Newell, 1996, J. Geophys. Res., 101, 2111~2134.

[19] Crawford, J. H D. D. Davis, G. Chen, J. Bradshaw, S. Sandholm, Y. Kondo, S. Liu, E. Browell, G. Gregory, B. Anderson, G. Sachse, J. Collins, J. Barrick, D. Blake, R. Talbot, and H. Singh, 1997, J. Geophys. Res., 102, 28469~28488.

[20] Crawford, J. H., D. D. Davis, G. Chen, J. Bradshaw, S. Sandholm, Y. Kondo, J. Merrill, S. Liu, E. Browell, G. Gregory, B. Anderson, G. Sachse, J. Barrick, D. Blake, R. Talbot, and R. Pueschel, 1997, J. Geophys. Res., 102, 28447~28468.

[21] Crawford, J. H., D. Davis, J. Olson, G. Chen, S. Liu, G. Gregory, J. Barrick, G. Sachse, S. Sandholm, B. Heikes, H. Singh, and D. Blake, 1999, J. Geophys. Res., 104, 16255~16273.

[22] Liss, P. S., and L. Merlivat, 1986, In The Role of Air-Sea Exchange in Geochemical Cycling, , D. Reidel, Mass., pp.113~127.

[23] Grodzinsky, G., D. Davis, G. Chen, Z.-H. Shon, A. Bandy, D. Thornton, F. Eisele, L. Mauldin, and D. Blake, 2000, accepted, Atmos. Env.

[24] Saltzman, E. S., D. B. King, K. Holmen, and C. Leck, 1993, J. Geophys. Res., 98, 16481~16486.

[25] Thompson A. M., J. E. Johnson, A. L. Torres, T. S. Bates, K. C. Kelly, E. Atlas, J. P. Greenberg, N. M. Donahue, S. Yvon, E. Saltzman, B. G. Heikes, B. W. Mosher, A. A. Shashkov, and V. I. Yegorov, 1993, J. Geophys. Res., 98, 16955~16968.

[26] Chen, G., unpublished results.

[27] Kettle, A. J., M. O. Andreae, D. Amouroux, t. W. Andreae, T. S. Bates, H. Berresheim, H. Bingemer, R. Boniforti, D. A. J. Curran, G. R. DiTullio, G. Helas, G. B. Jones, M. D. Keller, R. P. Kiene, C. Leck, M. Levasseru, G. Malin, M. Maspero, P. Matrai, A. R. McTaggart, N. Mihalopoulos, B. C. Nguyen, A. Novo, J. P. Putaud, S. Rapsomanikis, G. Roberts, G. Schebeske, S. Sharma, R. Simó, R. Staubes, S. Turner, and G. Uher, 1999, Global. Biogeo. Cycle, 13, 399~444.

[28] Wanninkhof, R., 1992, J. Geophys. Res., 97, 7373~7382.